The structure of PilA from *Acinetobacter baumannii* AB5075 suggests a mechanism for functional specialization in *Acinetobacter* type IV pili

Leslie A. Ronish[‡], Erik Lillehoj[§], James K. Fields[¶], Eric J. Sundberg[¶‖**], and ● Kurt H. Piepenbrink[‡ ‡‡§§¶¶1]

From the Departments of [‡]Biochemistry and [‡‡]Food Science and Technology, [§§]Nebraska Food for Health Center, and [¶¶]Center for Integrated Biomolecular Communication, University of Nebraska-Lincoln, Lincoln, Nebraska 68588 and the [¶]Institute of Human Virology and the Departments of [§]Pediatrics, [‖]Medicine, and [**]Microbiology and Immunology, University of Maryland School of Medicine, Baltimore, Maryland 21201

Edited by Chris Whitfield

Type IV pili (T4P) are bacterial appendages composed of protein subunits, called pilins, noncovalently assembled into helical fibers. T4P are essential, in many bacterial species, for processes as diverse as twitching motility, natural competence, biofilm or microcolony formation, and host cell adhesion. The genes encoding type IV pili are found universally in the Gram-negative, aerobic, nonflagellated, and pathogenic coccobacillus *Acinetobacter baumannii*, but there is considerable variation in PilA, the major protein subunit, both in amino acid sequence and in glycosylation patterns. Here we report the X-ray crystal structure of PilA from AB5075, a recently characterized, highly virulent isolate, at 1.9 Å resolution and compare it to homologues from *A. baumannii* strains ACICU and BIDMC57, which are C-terminally glycosylated. These structural comparisons revealed that PilA[AB5075] exhibits a distinctly electronegative surface chemistry. To understand the functional consequences of this change in surface electrostatics, we complemented a Δ*pilA* knockout strain with divergent *pilA* genes from ACICU, BIDMC57, and AB5075. The resulting transgenic strains showed differential twitching motility and biofilm formation while maintaining the ability to adhere to epithelial cells. PilA[AB5075] and PilA[ACICU], although structurally similar, promote different characteristics, favoring twitching motility and biofilm formation, respectively. These results support a model in which differences in pilus electrostatics affect the equilibrium of microcolony formation, which in turn alters the balance between motility and biofilm formation in *Acinetobacter*.

Type IV pili (T4P)[2] are bacterial appendages composed of protein subunits, called pilins, noncovalently assembled into helical fibers. These appendages are found in a wide range of eubacteria and are related structurally to type II secretion pseudopili, competence-induced pili, and archeal archaella (1–3). In many bacteria, these organelles are essential for processes as diverse as twitching motility, natural competence, biofilm or microcolony formation, and adhesion to biotic and abiotic surfaces. These systems are phylogenetically diverse and are commonly divided into type IVa (widely distributed), type IVb (primarily found in enteric bacteria), and, proposed recently, type IVc (tight adherence pili) (4). All type IV pilus systems contain genes encoding for a cytoplasmic AAA+ ATPase (PilB), an integral membrane protein (PilC), and at least two pilins (5–7). One pilin, the major pilin, makes up nearly the entirety (~99%) of the pilus, with the other subunits, minor pilins, being incorporated either at the tip (8) or scattered along the length (9).

Type IV pilin gene products are easily identified by their combination of an N-terminal signal peptide (which is removed by a specific protease prior to their incorporation into the pilus fiber) followed by a hydrophobic α-helix (serving as a transmembrane domain for pilins in the inner/plasma membrane) and finally a soluble region commonly referred to as the pilin headgroup. The vast majority of known pilin headgroup structures are similar; a single globular domain consisting of an N-terminal α-helix with a C-terminal β-sheet packed against it (10). However, the amino acid sequences of these pilin headgroups are so diverse that even structurally similar proteins have insignificant (~10–20%) sequence identities (11). Despite the variety of type IV pilin proteins, which include minor pilins with multidomain headgroups (8, 9), a given pilin gene within a given species is typically well-conserved with only the major pilin showing significant variation (12). Sequence diversity in the major pilin has typically been attributed to diversifying selection (13).

Acinetobacter baumannii, a Gram-negative, aerobic, nonflagellated coccobacillus, expresses type IV pili, which are essential for twitching motility and natural competence (14), and contribute to

host cell adherence (15). T4P are ubiquitous within the *Acinetobacter* genus, which contains environmental strains from soil and water, as well as commensal and pathogenic strains isolated from mammalian hosts, including humans (16–18). *A. baumannii* has recently gained notoriety as a source of hospital-acquired infections (19–21), particularly for military personal returning from the Middle East (hence the moniker "Iraqibacter") (22); however, several other species related to *A. baumannii*, often simply referred to as the "Ab group," are routinely isolated from nosocomial infections (23, 24). In particular the four related species of the *Acinetobacter calcoaceticus*–*A. baumannii* (Acb) complex (*A. baumannii*, *A. calcoaceticus*, *Acinetobacter pitti*, and *Acinetobacter nosocomialis*) are difficult to distinguish (25) and have all been found to be infectious in model systems (26).

The type IVa pili of *A. baumannii* and related species have diverse PilA proteins (both in amino acid sequence and *O*-linked glycosylation) that are unrelated to the overall taxonomy. In this paper, we compare the structure and function of pilin proteins from three strains of *A. baumannii*: (i) ACICU (also known as H34), an epidemic, multidrug-resistant strain belonging to the European clone II group that was isolated from cerebrospinal fluid in an outbreak in Rome in 2005 (27); (ii) BIDMC 57, a 2013 respiratory isolate from Beth Israel Deaconess Medical Center (Boston, MA) and sequenced at the Broad Institute (Cambridge, MA); and (iii) AB5075, which was isolated in 2008 from a osteomyelitis of the tibia by a group at the Walter Reed Army Institute of Research (Silver Spring, MD) (28) and found by those authors to be more virulent than other *A. baumannii* isolates. However, correlating pilus isotypes with phenotypic characteristics is complicated by the divergence between *pilA* genotype and *Acinetobacter* genetic diversity; by way of example, *A. calcoaceticus* PHEA-2 is an industrial wastewater isolate, but PilA[PHEA2] is 94% identical to PilA[ACICU].

Previously, we solved X-ray crystal structures of PilA, the major pilin protein, from two strains of *A. baumannii*: ACICU and BIDMC57 (15). PilA[ACICU] and PilA[BIDMC57] were much more similar to pilin structures from *Pseudomonas aeruginosa* and *Dichelobacter nodosus* than to each other, seemingly products of convergent evolution. We have proposed that this divergence within *A. baumannii pilA* genes could potentially be explained by specialization for aerobic or anaerobic environments caused by differences in the distribution of disulfide bonds; the solved structures of FimA, the *D. nodosus* major pilin, and PilA[BIDMC57] lack disulfide bonds at the C terminus typically found in pilins from Gram-negative bacteria.

However, a phylogenetic analysis of amino acid sequences from the major pilins of *A. baumannii*, *P. aeruginosa*, and *D. nodosus* showed three clusters, each containing sequences from multiple species (15). We chose to examine the structure of PilA from *A. baumannii* AB5075, a recently characterized and unusually virulent clinical isolate (28), both as a representative of this third taxonic group and because unlike PilA[ACICU] and PilA[BIDMC57], PilA[AB5075] is not natively C-terminally glycosylated. We have solved the X-ray crystal structure of PilA[AB5075] and, after comparing it to the other *Acinetobacter* PilA structures, found differences in surface electrostatics,

which suggest a mechanism for functional differentiation in T4P based on the structure of PilA. To test our hypothesis, we have complemented a *pilA* knockout strain of a model strain, *A. nosocomialis* M2, with the pilin genes from *A. baumannii* AB5075, ACICU, and BIDMC57 to directly compare the resulting phenotypes. Our results, described below, suggest that a functional trade-off may exist between the ability of *Acinetobacter* T4P to promote biofilm formation and to function in twitching motility.

Results

Acinetobacter pilA is highly variable and shows evidence of convergent evolution with type IV pilins from other species.

Type IV pili are found in a wide variety of bacteria and have been widely studied in Gram-negative infectious strains, particularly *Pseudomonas* and *Neisseria* species, which produce copious amounts of pili under laboratory conditions (46–51). We previously noted the similarity in structure between *A. baumannii* PilA proteins and the equivalent major pilin proteins in *P. aeruginosa* and *D. nodosus*. All three of these gammaproteobacteria species have been isolated from mammalian hosts, as well as soil, and typically present with persistent opportunistic infections rather than acute bacteremia (26, 52, 53). These phenotypic similarities suggest that functional similarities may also exist between the three T4P systems.
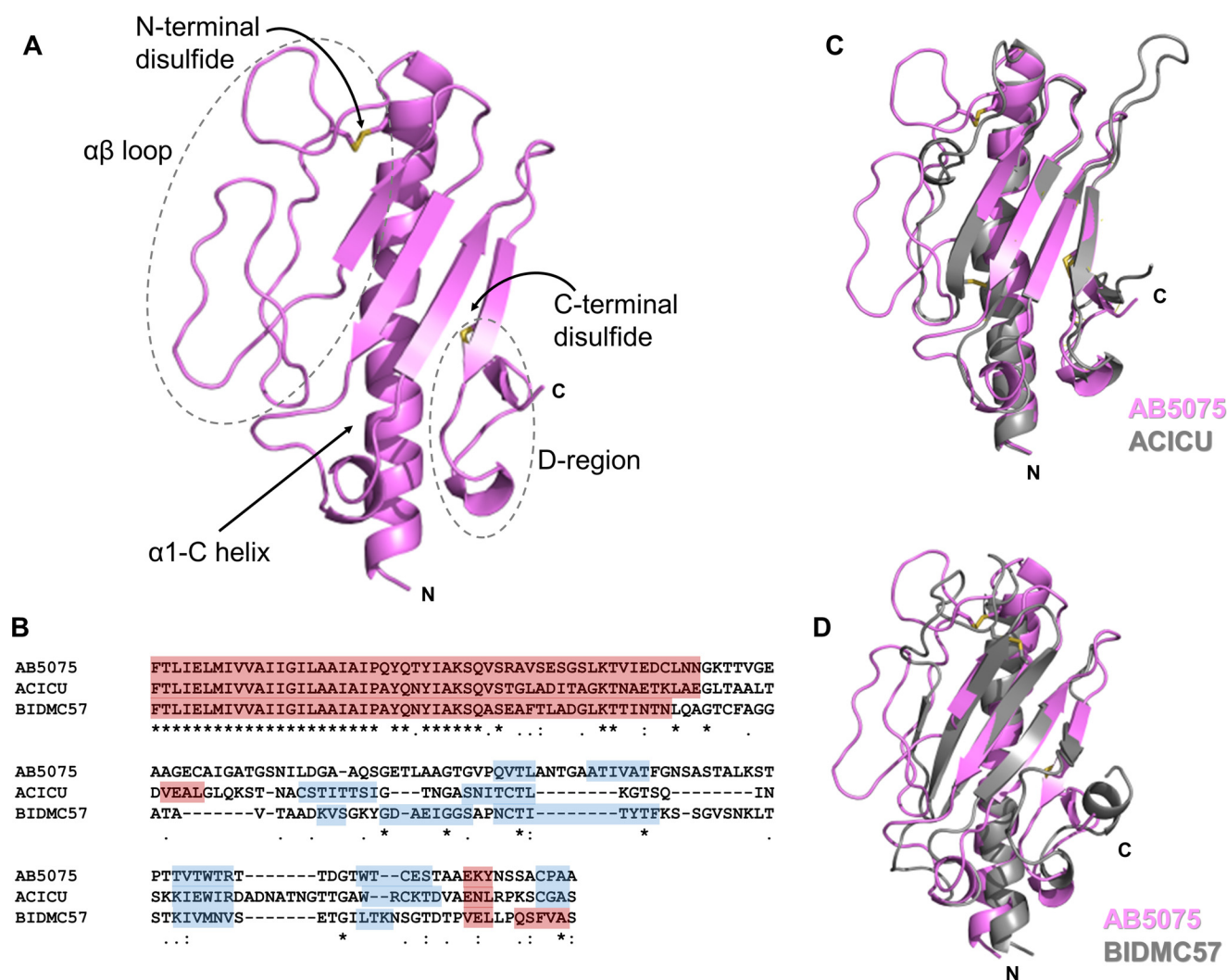
Fig. 1*A* shows a phylogenic tree of 60 *A. baumannii* PilA, *P. aeruginosa* PilA, and *D. nodosus* FimA amino acid sequences excluding the N-terminal signal peptides (all sequences begin FTLIEL...). The three branches of the unrooted tree each contain sequences from multiple species. On the *top left*, the branch containing PilA[ACICU] also contains *P. aeruginosa* PilA[PAO1] and PilA[PAK] among others. Counterclockwise, the next branch, containing PilA[BIDMC57], also includes *D. nodosus* FimA sequences from the predominant serotypes (A–C and E–G). The final branch contains representatives from all three species, including PilA[AB5075], *D. nodosus* FimA from serotypes D and H, and *P. aeruginosa* PilA[1244]. We noted the existence of this third branch in the dendogram previously (15). However, unlike the ACICU and BIDMC57 division, we could find no ready explanation for the division between the ACICU and AB5075 branches.

Notably, of the seven *A. baumannii* pilin genes, *pilA* alone shows this divergence, suggesting that the "machinery" of pilus assembly is conserved throughout. Fig. 1*B* shows a dendogram of the seven pilins from *A. baumannii* AB5075, ACICU, and BIDMC57. The *pilA* branch (circled in *red*) shows substantially more variation than the other six, which are well-conserved, particularly between ACICU and AB5075; in one case, PilV, the ACICU and AB5075 amino acid sequence are identical.

High-resolution structure of PilA[AB5075]

We determined the structure of PilA from *A. baumannii* AB5075 as a C-terminal fusion to maltose-binding protein to a resolution of 1.9 Å (Table 1). PilA[AB5075] possesses a typical type IVa pilin fold (Fig. 2*A*), beginning with an α-helix (α1-C, the N-terminal portion, residues 1–22, is hydrophobic and was removed for expression and crystallization), which leads into an

Figure 1. Phylogeny of *A. baumannii* type IV pilin genes. *A*, dendogram of major pilin amino acid sequences from 20 representative strains of *A. baumannii* (*green*), *P. aeruginosa* (*orange*), and *D. nodosus* (*blue*). The sequences of PilA[AB5075], PilA[ACICU], and PilA[BIDMC57] are marked on their respective branches (accession numbers in Table S1). *B*, dendogram of A. baumannii pilin amino acid sequences. Branches for each of the seven pilins are highlighted in *red* (PilA), *orange* (FimU), *light orange* (PilV), *yellow* (PilW), *green* (PilX), *light blue* (PilE1), and *dark blue* (PilE2); the genetic organization of the pilin genes is diagrammed below in the corresponding colors.

Table 1

Crystallographic parameters for MBP–PilA[AB5075]

The values in parentheses are for the highest resolution shell.

Resolution range	29.21–1.9 (1.968–1.9)
Space group	P 1 21 1
Unit cell	39.557, 103.04, 56.195, 90, 98.947, 90
Total reflections	156,212 (15709)
Unique reflections	34,906 (3467)
Multiplicity	4.5 (4.5)
Completeness (%)	99.64 (99.77)
Mean $I/\sigma(I)$	14.63 (2.44)
Wilson B-factor	28.44
R_{merge}	0.05718 (0.5332)
R_{pim}	0.02973 (0.28)
$CC_{1/2}$	0.999 (0.849)
CC^*	1 (0.958)
R_{work}	0.2002 (0.3110)
R_{free}	0.2432 (0.3382)
Root mean square	
Bonds	0.005
Angles	0.73
Ramachandran (%)	
Favored	97.70
Allowed	2.30
Outliers	0.00
Clashscore	4.04
Average B-factor	41.53
Macromolecules	41.45
Ligands	53.97
Solvent	42.23

extended loop (the $\alpha\beta$-loop, see below) and then a central β-sheet packed against the helix. Like PilA[ACICU] (and the majority of solved type IV pilin structures), one of its disulfide bonds is at the C terminus between the final two β-strands of

the central β-sheet, between residues 135 and 148. This similarity in disulfide bonding may explain why, despite the poor sequence conservation between the PilA[ACICU] and PilA[AB5075] C termini, their D-regions (the loops bound by the C-terminal disulfide bonds) are superimposable (Fig. 2C), unlike the equivalent C-terminal region of PilA[BIDMC57] (Fig. 2D). This supports our hypothesis that the C-terminal structure of PilA[BIDMC57] and the structurally similar *D. nodosus* FimA (serotype A, PDB ID: 3SOK) (54) contain C-terminal helices and hydrophobic regions to stabilize them in the absence of the disulfide bond. Previously we showed that alanine mutations of those C-terminal hydrophobic residues destabilized PilA[BIDMC57] (15). Fig. 2B shows a sequence alignment of PilA[AB5075], PilA[ACICU], and PilA[BIDMC57]; despite the structural conservation in the central β-sheet, the sequence similarity is low: ~35% for any of the three to either of the other two, excluding the N-terminal transmembrane helix (residues 1–22).

The most striking feature of the PilA[AB5075] structure is the $\alpha\beta$-loop (from the end of the central α-helix to the start of the first β-strand in the central β-sheet); bounded by a *dashed gray line* in Fig. 2A. Approximately 15 residues longer than the $\alpha\beta$-loop of PilA[ACICU], it contains a disulfide bond to the central α-helix (residues 50 and 65) and twists back over itself twice, extending out from the center of the headgroup. It contains none of the α-character found in the ACICU $\alpha\beta$-loop but has some positional overlap with the BIDMC57 $\alpha\beta$-loop (Fig. 2)

Figure 2. Structure of PilA^AB5075. *A*, cartoon representation of PilA^AB5075 headgroup; disulfide bonds are displayed in *yellow*. *B*, sequence alignment of PilA^AB5075, PilA^ACICU and PilA^BIDMC57. α-Helices are highlighted in *red*, and β-strands are in *blue*. Sequence identity (*), close similarity (:), and similarity (.) are indicated below. *C*, superimposition of PilA^AB5075 (*pink*) and PilA^ACICU (*gray*). *D*, superimposition of PilA^AB5075 (*pink*) and PilA^BIDMC57 (*gray*).
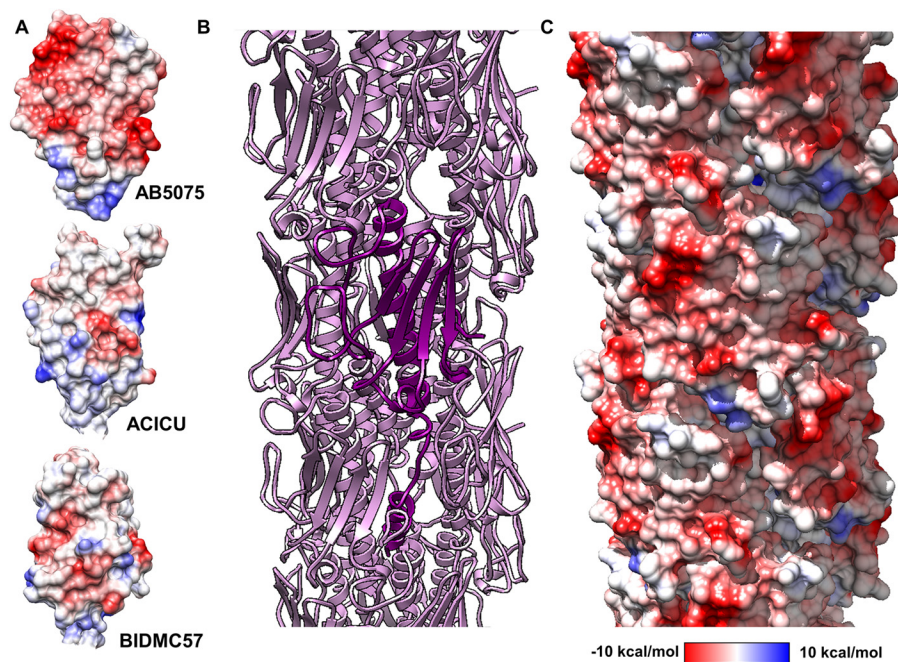
and the pilin of *P. aeruginosa* PAK (36). Despite the long stretches with no α- or β-structure, the loop conformation can be unambiguously determined because of the well-defined electron density in this region (Fig. S1). An analysis of relative B-factors for PilA^AB5075, PilA^ACICU, and PilA^BIDMC57 suggests that the internal dynamics of PilA^AB5075 and PilA^ACICU may be similar as well (Fig. S2). Both have relatively low b-factors for the α1-C helix and central β-sheet with intermediate relative b-factors for the αβ-loop (though higher for two of the loops in PilA^AB5075) and the highest relative b-factors at the C terminus. Conversely, PilA^BIDMC57 has a gradient of relative b-factors running along the α1-C helix from the N-terminal portion (low) to the tip and αβ-loop (high), whereas the C terminus is relatively well-ordered.

Surface electrostatics of A. baumannii PilA variants

Variation in the αβ-loop of pilin proteins is well-documented (10), but the unusual structure of the αβ-loop in PilA^AB5075 suggested some functional role to us. An examination of the surface electrostatics of PilA^AB5075 showed an unusual concentration of acidic groups at the surface, particu-

larly in the αβ-loop itself (Fig. 3A). The contrast is particularly striking with PilA^ACICU. Calculations of theoretical isoelectric points for the two headgroups (*i.e.* excluding residues 1–22) give values of 4.73 for PilA^AB5075 and 8.43 for PilA^ACICU. To evaluate the implications of the extended αβ-loop and its electronegative surface for a native pilus, we created models of full-length PilA^AB5075 (that is modeling the transmembrane helix spanning residues 1–22) (Fig. S3A) and an assembled AB5075 type IV pilus based on the 2006 model *Neisseria gonorrhoeae* pilus (37) (Fig. S3B) and the higher-resolution 2017 *P. aeruginosa* model from Wang *et al.* (55) (Fig. 3B and Fig. S3C). Electronegativity clearly predominates, with the few electropositive regions on the surface confined to a recessed groove, which follows the helical symmetry axis around the pilus fiber (Fig. 3C and Fig. S3D).

If we compare the charged residues that are exposed on the surface of the AB5075 and ACICU pilus models (Fig. S4), each has six negatively charged (aspartate or glutamate) residues, but the ACICU surface also contains seven positively charged (lysine or arginine) residues, whereas none are found on the

Figure 3. Model of the *A. baumannii* AB5075 type IV pilus. *A*, columbic surfaces of the PilA[AB5075], PilA[ACICU], and PilA[BIDMC57] headgroups. *B*, cartoon representation of pilus model (*pink*). A single modeled full-length pilin is depicted in *violet*. *C*, columbic electrostatic surface depiction of the AB5075 pilus. Electrostatic potential key for *A* and *C* is shown below.

equivalent AB5075 surface (lysine 117 can be found in the previously mentioned groove). Two of these basic surface residues form unambiguous salt bridges with acidic residues (lysine 69/glutamate 63 and arginine 122/aspartate 109), whereas three other pairs are within 3 Å but ambiguous from the side-chain density (lysine 102/aspartate 126, lysine 103/glutamate 105, and arginine 132/glutamate 129). One logical consequence of an increased electronegativity of the pilus surface is that electrostatic repulsion would then disfavor pilus–pilus contacts, including the formation of pilus bundles, which have been demonstrated to promote microcolony formation in type IVb pili (56, 57).

Twitching motility by Δ*pilA* complements

Phenotypic comparisons of *A. baumannii* have been undertaken by several other groups previously (58–60). Eijkelkamp *et al.* (60), in particular, examined the correlation between *pilA* sequence and motility and biofilm phenotypes, finding a link between *pilA* sequence and twitching motility. In this study, because we wished to isolate the effects of variation in PilA from other factors, we introduced *pilA* genes from *A. baumannii* AB5075, ACICU, and BIDMC57 into a Δ*pilA* strain of *A. nosocomialis* M2. This strain, originally described as *A. baumannii* M2 (14), has been used as a model system for studies of multiple aspects of *Acinetobacter* pathogenesis (15, 21, 61).
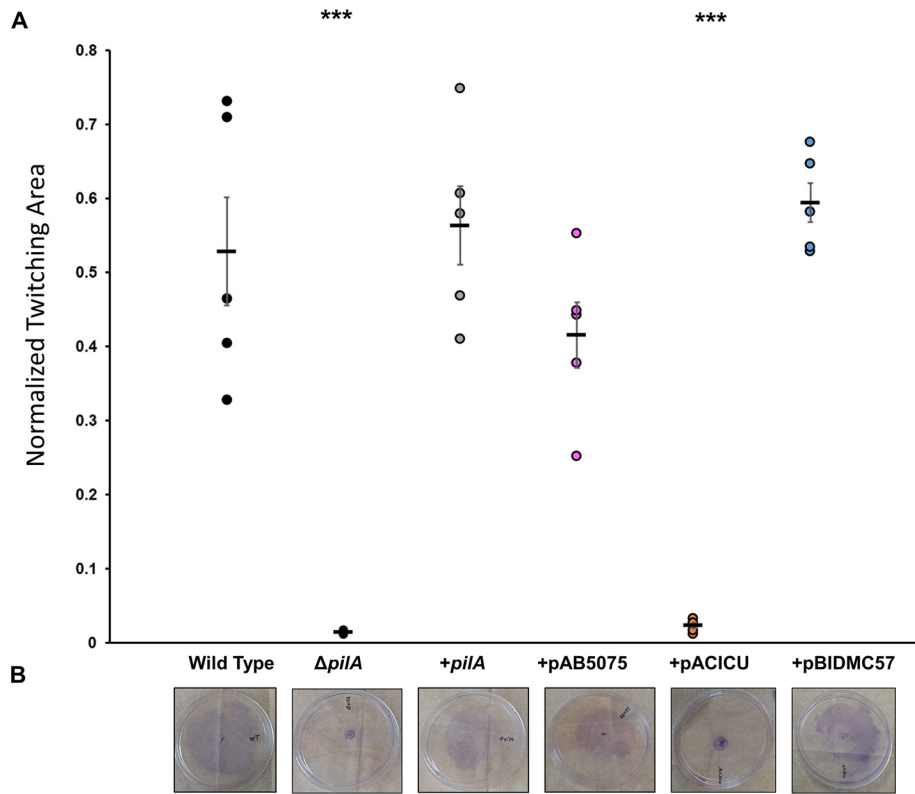
We measured the ability of *A. nosocomialis* M2 Δ*pilA* complemented with plasmids containing *pilA* from *A. baumannii* AB5075, ACICU, and BIDMC57 (Fig. S5), as well as positive and negative controls to move at the interface between nutrient agar and polystyrene using standard methods (14). To quantitate the extent of twitching motility, we used crystal violet to stain the bacteria and image analysis software to distinguish bacteria from background and using WT, Δ*pilA*, Δ*pilT*, and

complements for validation (Fig. S6). The results from 1% MacConkey agar plates (Fig. 4) show that the AB5075 and BIDMC57 complements were able to complement the Δ*pilA* phenotype with much greater effectiveness than the ACICU mutant. The ACICU mutant did show significantly more movement than Δ*pilA* ($p = 0.035$) but was at least an order of magnitude worse than the WT, native complement, AB5075 complement, and BIDMC57 complement.

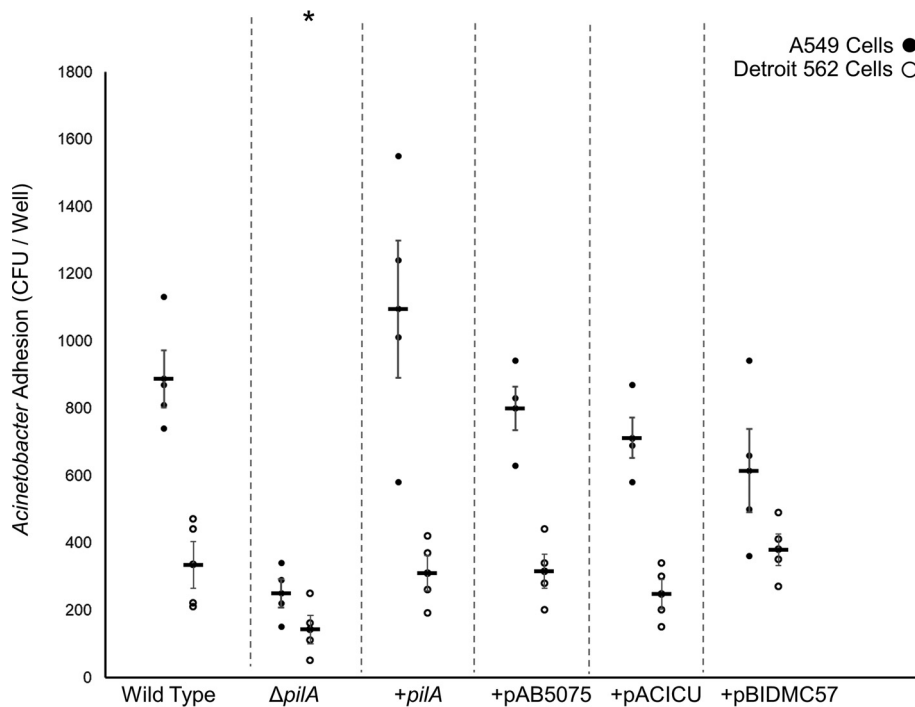### Adhesion to A549 and Detroit 562 cells

Previously we reported that the Δ*pilA* mutant of *A. nosocomialis* M2 showed a defect in adhesion to A549 cells, an immortalized cell line derived from lung epithelial cells, which was restored in the complemented strain (15). Additionally, adhesion was significantly increased in the Δ*pilT* mutant, which is incapable of retracting type IV pili. Based on these results, we reasoned that if the *pilA*[ACICU] complement was poorly motile because it produced few T4P, it would correspondingly be a poor complement for the native pilin in these host cell adhesion assays. If, however, the *pilA*[ACICU] complement was capable of normal pilus biogenesis but incapable of retraction, similar to what was observed previously by Rogers *et al.* (79), we would expect it to adhere to A549 cells more strongly than the *pilA*[AB5075] and *pilA*[BIDMC57] complements.

These assays were performed as described previously (15) with the exception that the bacteria were grown in MacConkey medium rather than Luria broth (see "Experimental procedures"). This change was prompted by our observation that type IV pilus expression by *A. nosocomialis* M2, as evidenced by twitching motility, is significantly greater in MacConkey medium than in Luria broth (Fig. S7). The results (Fig. 5) show that under these conditions, robust binding to both A549

A

B

Figure 4. Twitching motility of *A. nosocomialis* M2 and complemented strains. *A*, normalized twitching area, expressed as the fraction of the plate covered. *Error bars* represent standard error. ***, $p < 0.001$. *B*, representative images of twitching results after staining with crystal violet.
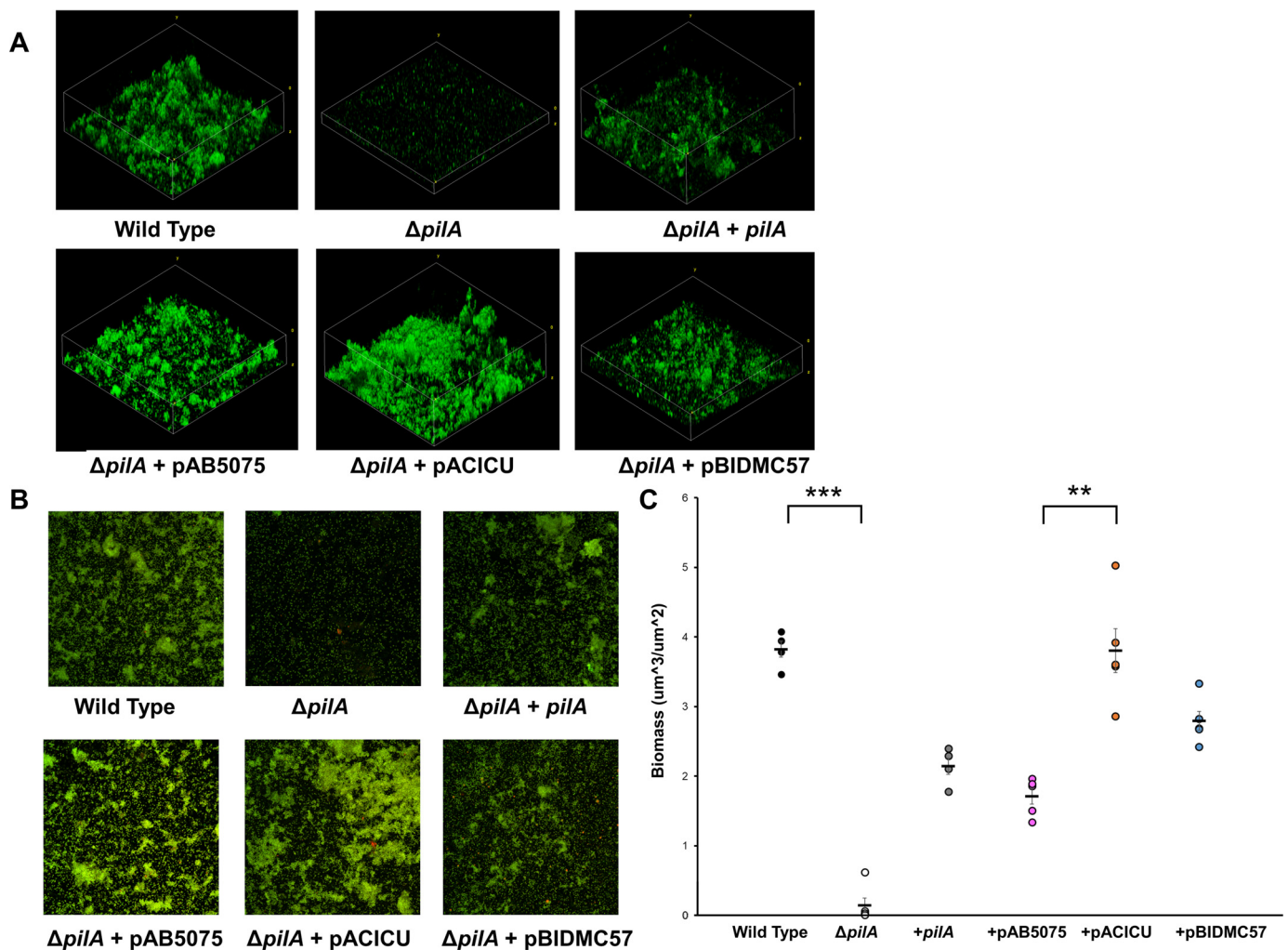

Figure 5. Host cell adherence through *Acinetobacter* type IV pili. The average number of cfu of *A. nosocomialis* recovered from a binding experiment with either A549 cells (*black circles*) or Detroit 562 cells (*white circles*) is shown. *Error bars* represent standard error. Significant ($p < 0.05$) reduction for both cell lines is marked with an *asterisk* (*).

and Detroit 562 (nasopharyngeal) cells is observed for the WT strain and significantly decreased in the Δ*pilA* mutant and that all three of *A. baumannii pilA* complements restore adhesion with no significant differences between them.

These data indicate that all three *pilA* complements are capable of both extension and retraction of T4P, and we find no relationship between PilA sequence and the relative binding to these two cell types.

Figure 6. Acinetobacter biofilm formation on stainless steel. *A*, 3D reconstructions of biofilms imaged by CLSM. *B*, 2D, top-down CLSM images. *C*, biofilm biomass calculated for *A. nosocomialis* M2, Δ*pilA*, and complements. *Error bars* represent standard error. **, $p < 0.01$; ***, $p < 0.01$.
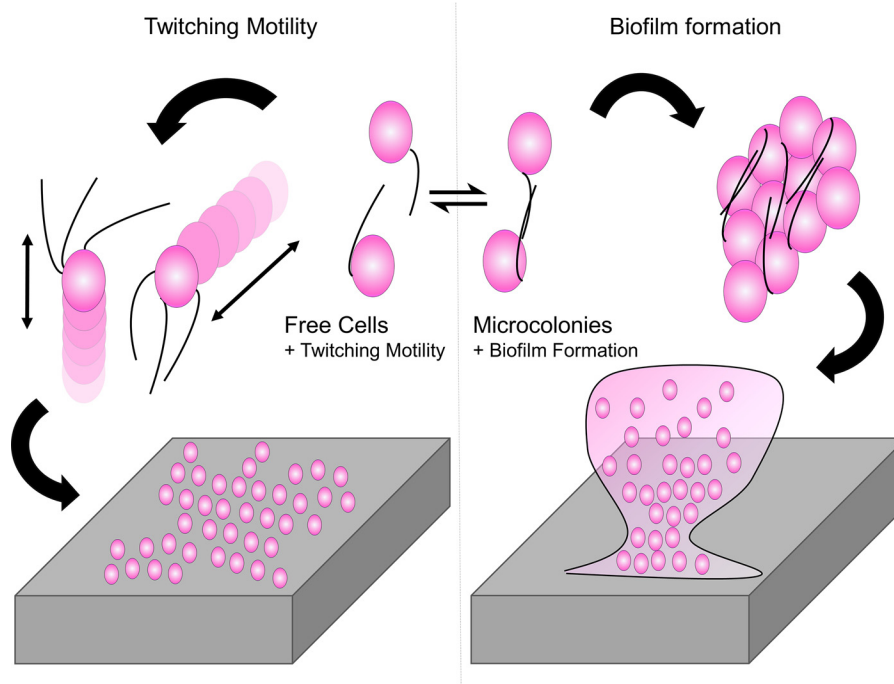
A. baumannii biofilm formation on stainless steel

If the divergence in PilA sequence is the result of functional specialization, we would expect that a defect in one function would be compensated for by a gain in another. Correspondingly, we also measured the ability of our complements to form biofilm in a vertical biofilm formation assay similar to a CDC biofilm reactor (62). Briefly, sterilized stainless steel coupons were placed upright in culture tubes and immersed in MacConkey medium, and the medium was inoculated with bacterial cultures from saturation growths. Our experimental design was influenced by several factors, including our prior results growing biofilms horizontally on glass surfaces (15). Previously we found no significant difference between *A. nosocomialis* M2 WT, Δ*pilA*, and the native complement in biofilm formation on horizontal glass surfaces grown in Luria broth. However, as noted above, we now expected stronger T4P-dependent phenotypes in MacConkey medium. Similarly, *Acinetobacter* adhesion to stainless steel is well-characterized and robust compared with untreated glass (63). We attribute the growth medium dependence of T4P expression to differences in the production of quorum-sensing molecules, consistent with the observation that virstatin (an inhibitor of AnoR/AnoI)

reduces both surface motility and biofilm formation in *A. baumannii* (64, 65).

After fixation and fluorescent staining with FM 1–43, biofilm formation was assessed using confocal laser scanning microscopy (CLSM) (Fig. 6). Calculated biomass shows a significant phenotype for the Δ*pilA* mutant, which can be complemented by the native M2 *pilA* gene as well as the *pilA* genes of AB5075, ACICU, and BIDMC57. Additionally, the ACICU complement formed significantly greater biomass than the AB5075 complement (Fig. 6C). We attribute this difference in biomass to differences in bacterial aggregation because all strains, including Δ*pilA*, were able to adhere in a monolayer to the stainless steel surface (Fig. 6B). Additionally, we found that biofilm formation was accompanied by the formation of cross-linking pilus-like fibers for all strains (Fig. S8), which we attribute to chaperone-usher (Csu) pili, consistent with their role in *Acinetobacter* biofilm formation (66, 67).

Discussion

Variation in the genetics of *A. baumannii* virulence factors, including type IV pili, is well-established, and with the improvements in metagenomics sequencing technology, the acquisition

Figure 7. Schematic model for specialization in *Acinetobacter* type IV pili. A potential tradeoff between biofilm formation and twitching motility based solely on PilA structure is depicted based on the equilibrium between singled and bundled T4P.

of genomic data continues to accelerate. In this work we examine the relationships between genetic variation in the major subunit of type IV pili, PilA, the molecular structure of type IV pili, and the resulting bacterial phenotypes. We observed differences in surface chemistry between PilA^{AB5075} and PilA^{ACICU} even as the secondary structure was largely conserved and found that the two proteins promoted different bacterial behavior as well, with the AB5075 pilin favoring motility and the ACICU pilin favoring biofilm formation. We propose that these results can be explained by the equilibrium between single and bundled type IV pili.

Type IV pili mediate diverse functions in a variety of bacteria (10), but all of the known functions rely on some interplay between two general characteristics: adhesion (whether to DNA, biotic or abiotic surfaces, or each other) (56) and retraction (which is essential for twitching motility and natural competence) (14). The stark contrast in surface electrostatics between PilA^{AB5075} and PilA^{ACICU}, given the overall similarity in fold, suggested to us that fibers formed from PilA^{AB5075} would be more prone to electrostatic repulsion and hence adhere less to each other.

Pilus bundling has also been shown to be a function of pilin surface chemistry; *Neisseriae* type IV pili are less bundled when glycosylated at serine 63 (68, 69). Because, unlike *A. baumannii* AB5075, the ACICU and BIDMC57 strains C-terminally glycosylate PilA, they may reduce pilus bundling through glycosylation without the need for electrostatic repulsion. However, it is important to distinguish between bundling between the pili of a single cell (*cis*-bundling) and bundling between the pili of adjacent cells (*trans*-bundling). *cis*-Bundling is no detriment to motility and in fact has been shown to dramatically increase force of pilus retraction and to increase the persistence of twitching motility (70, 71).

Trans-bundling promotes microcolony formation in enteropathogenic *Escherichia coli* and *Vibrio cholerae* (56, 57), a precursor to biofilm formation. The balance between *cis-* and *trans*-bundling is also dependent upon the number of pili per cell, which is dramatically lower in *Acinetobacter* than *Neisseriae* and *Pseudomonas* (14, 37, 55).

An increase in microcolony formation could explain both the greater biofilm formation of the ACICU complement and its poor motility. A scheme describing this model is shown in Fig. 7. Single cells are free to move across the surface, resulting in an overall increase in twitching motility, whereas cells joined together into microcolonies are less motile but serve as nucleants for the formation of biofilm.

Inverse relationships between twitching motility and biofilm formation have been observed previously in *P. aeruginosa* Δ*pilT* mutants (38) and correlatively in clinical isolates (72). In cases where Δ*pilT* mutants are hyperpilated, increases in retraction-independent adhesive functions can be explained simply through the increase in adhesive molecules on the surface. By way of example, we previously reported increased host cell adhesion for the *A. nosocomialis* M2 Δ*pilT* mutant (15). However, we observe no hyperpilation of the *pilA*^{ACICU} complement, either directly by TEM (Fig. S9) or in increased host cell adhesion (Fig. 5), implying that the defect in motility does not stem directly from decreased pilus retraction.

Returning to prior studies comparing the phenotypes of *A. baumannii* strains, we examined the degree to which the results reported here were consistent with the behavior of the native bacteria. Eijkelkamp *et al.* (60) compared the motility and adhesion characteristics of a wide variety of clinical isolates and reported that only 3 of 32 international clone II isolates (which includes ACICU) showed twitching motility, in contrast to international clone I (which have *pilA* sequences similar to

AB5075), in which 8 of 8 were motile; this correlation between PilA sequence and motility was also noted by the authors. However, although these results are consistent with what we observe with the *pilA*^AB5075^ and *pilA*^ACICU^ complements, we note that American Type Culture Collection 19606, which has a *pilA* sequence very similar to BIDMC57, was found to be nonmotile in that study. More recently and also consistent with our findings, Sahl *et al.* (73) found greater biofilm formation by ACICU than AYE (which has a PilA sequence identical to AB5075).

If a tradeoff between twitching motility and biofilm formation can explain the differentiation of *Acinetobacter* type IV pili, what evolutionary pressures favor one over the other? Because the three pilin proteins in this study are from *A. baumannii* clinical isolates, one obvious possibility is that differences in infection sites led to specialist pathogens. This view is supported by the observation by Vijayakumar *et al.* (72) that *A. baumannii* isolates from the sputum formed more biofilm *in vitro* than isolates from the blood, whereas the reverse was true for twitching motility. However, *Acinetobacter* strains with similar type IV pilins have also been isolated environmentally; *A. calcoaceticus* PHEA-2 has a PilA sequence nearly identical to that of *A. baumannii* ACICU (94% amino acid identity) but was isolated from industrial wastewater (74). It is possible that a distinction exists between the T4P of environmentally adapted strains, which retain some infectivity and the T4P of specialized pathogenic strains; Wang *et al.* (75) observed a trend associating biofilm-forming strains with better clinical outcome. However, more work comparing clinical, commensal, and environmental isolates in controlled studies, particularly models of infection, remains to be done before we can draw such a conclusion.

The ability of all three *A. baumannii pilA* complements to adhere to host cells in a similar manner despite their differences in structure and surface chemistry is consistent with our prior observation that the removal of a C-terminal pentasaccharide from the *A. nosocomialis* PilA protein also has no effect on binding to A549 or Detroit 562 cells. We hypothesize that the relevant adhesin in this case is not PilA itself but a minor pilin subunit (consistent with the conservation we see of the minor *A. baumannii* minor pilins in Fig. 1) or a protein that interacts with the pilus, either constitutively at the tip (76) or as a secreted factor, as was recently shown in the type IVb pili of ETEC (77).

Recently, Harvey *et al.* (78) reported that pilus glycosylation can inhibit the binding of phage to the type IV pili of *P. aeruginosa*, providing the most compelling explanation to date for the wide prevalence of pilin glycosylation. With that in mind, we considered the possibility that the electronegative surface chemistry of PilA^AB5075^ could also be explained in terms of defense against phage (PilA^AB5075^ is not C-terminally glycosylated, unlike PilA^ACICU^ and PilA^BIDMC57^). However, based on the available structures of *Pseudomonas* PilA proteins that are not natively glycosylated, pronounced surface electronegativity does not appear to be a general feature of pilins lacking C-terminal glycans.

In conclusion, the results here demonstrate that subsets of *A. baumannii* produce type IV pili with markedly different molecular structure, and this variation, particularly in terms of

surface chemistry, can result in phenotypic differences in motility and biofilm formation. The prevalence of type IV pili, in general, and the homology between *A. baumannii* type IV pili and those of phenotypically similar species such as *P. aeruginosa*, in particular, imply that these findings may be generalizable to other biofilm-forming bacteria.

Experimental procedures

Protein expression and purification

PilA^AB5075^ was expressed and purified as described previously (15). Briefly, the codon-optimized sequence, starting with alanine 23, was cloned into a maltose-binding fusion vector under a T7 promoter, making use of previously described surface entropy reduction mutations (pMal E) (29). A C-terminal His$_6$ tag was included to ease purification. This plasmid was transformed into BL21 (DE3) pLysS cells and grown to saturation overnight with shaking at 37 °C in LB medium with 50 μg/ml ampicillin. These saturation cultures were then diluted into fresh LB-ampicillin and grown with shaking to an optical density of 0.5 at 37 °C. The flasks were cooled to 18 °C before induction with 30 mM isopropyl β-D-1-thiogalactopyranoside and allowed to grow overnight with shaking before being harvested by centrifugation at 7,500 $\times$ g for 10 min. The cells were lysed using lysozyme (0.25 mg/ml final concentration), DNase (0.02 mg/ml) and Triton X-100 (0.5%) for 10 min, and the resulting lysate was centrifuged again, this time at 20,000 $\times$ g for 30 min. The supernatant was purified using a nickel–nitrilotriacetic acid column, and the elution was further purified through size-exclusion chromatography over a GE S200 Superdex column using an Äkta Purifier FPLC.

Structure determination and refinement

Maltose-binding protein–PilA^AB5075^ crystallization conditions were screened by sitting-drop vapor diffusion at a concentration of 20 mg/ml in 20 mM Bis-Tris (pH 6.0), with and without 50 mM maltose. A crystallization condition was found, without the addition of maltose, in the Morpheus screen (Molecular Dimensions), (H4), 12.5% (w/v) PEG 1000, 12.5% (w/v) PEG 3350, 12.5% (v/v) 2-methyl-2,4-pentanediol, 0.02 M of amino acid mix (0.2 M DL-glutamatic acid monohydrate, 0.2 M DL-alanine, 0.2 M glycine, 0.2 M DL-lysine monohydrochloride, and 0.2 M DL-serine), 0.1 M MES/imidazole, pH 6.5. Crystals were grown in hanging drops at room temperature and took ~48 h to grow at a protein concentration of 10 mg/ml. They were then harvested and flash-cooled in the mother liquor supplemented with 20% ethylene glycol. The data were collected at the Advanced Photon Source, GM/CA, Beamline 23ID-D. The General Medical Sciences and Cancer Institutes of Structural Biology Facility at the Advanced Photon Source (GM/CA @ APS) is a part of the X-ray Science Division at APS, Argonne National Laboratory (ANL).

The resulting data set was processed with XDS. Molecular replacement was carried out by Phaser (30) using a sequential search of (i) maltose-binding protein and (ii) PilA from *A. baumannii* ACICU (15). Phenix and Coot were used for phasing, building, and refinement (31–34). The crystallographic parameters of the refined data are summarized in Table 1.

Electrostatic calculations

Columbic surfaces were calculated using UCSF Chimera (35) using a distance-dependent dielectric and a dielectric constant of 4.0, 1.4 Å from the surface. Theoretical polypeptide isoelectric points were calculated using The Swiss Institute of Bioinformatics (ExPASy) ProtParam server (https://web.expasy.org/protparam/).

Pilus modeling

Full-length PilA^{AB5075} was modeled based on the structure of the full-length *P. aeruginosa* PAK pilin (36). The initial model of the pilus was created by superimposition onto a model of the *N. gonorrhoeae* type IV pilus filament (Protein Data Bank code 2HIL) (37). The resulting model was then minimized using UCSF Chimera (35).

Complementation of pilA mutant

pilA genes from *A. baumannii* AB5075, ACICU, and BIDMC57 were synthesized (Genscript) and ligated into pUCP20GM (38) using BamH1 and HindIII restriction sites (accession numbers in Table S1). The resulting vectors were electroporated into *A. nosocomialis* M2 Δ*pilA* (14) using standard protocols (39). The presence of the plasmids was confirmed by both resistance to gentamycin and PCR of the pilin genes.

Twitching motility

A. nosocomialis M2 (including mutants and complement strains) was grown on 1.5% MacConkey agar plates overnight. Colonies were selected and stabbed through the centers of 1% agar plates in polystyrene Petri dishes. The plates were incubated in sealed bags at 37 °C for 3 days. The agar was then removed, and the bacteria which adhered to the polystyrene Petri dish were stained with 0.1% crystal violet for 5 min. Excess crystal violet was removed by gentle washing with deionized water. The subsurface twitching area on each plate was accessed using GIMP imaging software. Statistics were calculated for five replicates and significance determined by Student's *t* test.

Biofilm formation

All strains were grown on 1.5% MacConkey agar plates, supplemented when necessary with gentamycin for plasmid maintenance. Overnight cultures were grown from these plates in MacConkey medium and diluted 1:10 into fresh MacConkey medium in 10-cm^2 flat tissue culture tubes (TPP Techno Plastic Products AG) containing upright 1/8 × 1-inch untreated stainless steel fender washers (Everbilt). After 72 h of shaking (50 rpm) at room temperature, the washers were removed to 6-well cell-culture plates, gently washed with PBS, stained, and covered in aluminum foil, with FM 1–43 dye (1:1000 in PBS) for 15 min at room temperature. The samples were then washed with PBS and fixed overnight with 4% paraformaldehyde in PBS at 4C. The fixed samples were stored at 4 °C in PBS until being imaged as described below.

Confocal laser scanning microscopy

Biofilms were grown on stainless steel surfaces and prepared as described above. Each stainless steel washer was covered with a 18 × 18-mm glass coverslip and read using a Nikon A1 confocal laser scanning microscope and accompanying software (Nikon, Tokyo, Japan). *Z*-stacks were acquired for each strain. The structural organization of the biofilms was analyzed using the Comstat2 software package (http://www.comstat.dk)[3] (40). The 3D representations of the biofilms were generated using the 3D viewer plugin for the FIJI distribution of ImageJ (http://3dviewer.neurofly.de)[3] (41).

Cell adhesion

A549 human airway adenocarincoma cells (52) (American Type Culture Collection, CCL 185) or Detroit 562 pharyngeal carcinoma cells (53) (American Type Culture Collection, CCL 138) were seeded in 24-well culture plates and cultured at 37 °C, 5% CO_2 to 2.0×10^5 cells/well in Dulbecco's modified Eagle's medium containing 10% fetal bovine serum, 2.0 mM glutamine, 100 units/ml penicillin, and 100 µg/ml streptomycin. The cells were washed twice with PBS, pH 7.2, fixed for 10 min at room temperature with 2.5% (v/v) glutaraldehyde in PBS, pH 7.2, and washed three times with PBS, pH 7.2, as described (42, 43). *A. nosocomialis* M2 (including mutants and complements) was cultured overnight in MacConkey broth, washed twice with PBS, pH 7.2, resuspended in PBS, pH 7.2 containing 2.0 mg/ml glucose, and quantified spectrophotometrically at A_{600}. Fixed A549 or Detroit 562 cells (2.0×10^5/well) were incubated with 2.0×10^7 cfu/well of *A. nosocomialis* M2 in 0.5 ml for 40 min at 37 °C and washed three times with PBS, pH 7.2. Bound bacteria were released with 0.05% trypsin-EDTA, and bound colony-forming units were quantified on Luria Bertani agar plates, as described (42, 43). Significance was determined by Student's *t* test.

All depictions of protein structures were created using PyMOL (Schrödinger) or UCSF Chimera (35). Sequence alignments were made using Clustal Omega (44), and phylogenic trees were diagrammed using Interactive tree of life (iTOL) from EMBL (45).

References

1. Muschiol, S., Erlendsson, S., Aschtgen, M. S., Oliveira, V., Schmieder, P., de Lichtenberg, C., Teilum, K., Boesen, T., Akbey, U., and Henriques-Normark, B. (2017) Structure of the competence pilus major pilin ComGC

---

[3] Please note that the JBC is not responsible for the long-term archiving and maintenance of this site or any other third party hosted site.

ⓈASBMB

J. Biol. Chem. (2019) 294(1) 218–230 **227**

in *Streptococcus pneumoniae*. *J. Biol. Chem.* **292,** 14134–14146 CrossRef Medline

2. Shahapure, R., Driessen, R. P., Haurat, M. F., Albers, S. V., and Dame, R. T. (2014) The archaellum: a rotating type IV pilus. *Mol. Microbiol.* **91,** 716–723 CrossRef Medline

3. Johnson, T. L., Abendroth, J., Hol, W. G., and Sandkvist, M. (2006) Type II secretion: from structure to function. *FEMS Microbiol Lett.* **255,** 175–186 CrossRef Medline

4. Ellison, C. K., Kan, J., Dillard, R. S., Kysela, D. T., Ducret, A., Berne, C., Hampton, C. M., Ke, Z., Wright, E. R., Biais, N., Dalia, A. B., and Brun, Y. V. (2017) Obstruction of pilus retraction stimulates bacterial surface sensing. *Science* **358,** 535–538 CrossRef Medline

5. Giltner, C. L., Nguyen, Y., and Burrows, L. L. (2012) Type IV pilin proteins: versatile molecular modules. *Microbiol. Mol. Biol. Rev.* **76,** 740–772 CrossRef Medline

6. Strom, M. S., and Lory, S. (1993) Structure-function and biogenesis of the type IV pili. *Annu. Rev. Microbiol.* **47,** 565–596 CrossRef Medline

7. Craig, L., Pique, M. E., and Tainer, J. A. (2004) Type IV pilus structure and bacterial pathogenicity. *Nat. Rev. Microbiol.* **2,** 363–378 CrossRef Medline

8. Ng, D., Harn, T., Altindal, T., Kolappan, S., Marles, J. M., Lala, R., Spielman, I., Gao, Y., Hauke, C. A., Kovacikova, G., Verjee, Z., Taylor, R. K., Biais, N., and Craig, L. (2016) The *Vibrio cholerae* minor pilin TcpB initiates assembly and retraction of the toxin-coregulated pilus. *PLoS Pathog.* **12,** e1006109 CrossRef Medline

9. Piepenbrink, K. H., Maldarelli, G. A., de la Peña, C. F., Mulvey, G. L., Snyder, G. A., De Masi, L., von Rosenvinge, E. C., Günther, S., Armstrong, G. D., Donnenberg, M. S., and Sundberg, E. J. (2014) Structure of *Clostridium difficile* PilJ exhibits unprecedented divergence from known type IV pilins. *J. Biol. Chem.* **289,** 4334–4345 CrossRef Medline

10. Craig, L., and Li, J. (2008) Type IV pili: paradoxes in form and function. *Curr. Opin. Struct. Biol.* **18,** 267–277 CrossRef Medline

11. Piepenbrink, K. H., Maldarelli, G. A., Martinez de la Peña, C. F., Dingle, T. C., Mulvey, G. L., Lee, A., von Rosenvinge, E., Armstrong, G. D., Donnenberg, M. S., and Sundberg, E. J. (2015) Structural and evolutionary analyses show unique stabilization strategies in the type IV pili of *Clostridium difficile*. *Structure* **23,** 385–396 CrossRef Medline

12. Cehovin, A., Winterbotham, M., Lucidarme, J., Borrow, R., Tang, C. M., Exley, R. M., and Pelicic, V. (2010) Sequence conservation of pilus subunits in *Neisseria meningitidis*. *Vaccine* **28,** 4817–4826 CrossRef Medline

13. Toma, C., Kuroki, H., Nakasone, N., Ehara, M., and Iwanaga, M. (2002) Minor pilin subunits are conserved in *Vibrio cholerae* type IV pili. *FEMS Immunol. Med. Microbiol.* **33,** 35–40 CrossRef Medline

14. Harding, C. M., Tracy, E. N., Carruthers, M. D., Rather, P. N., Actis, L. A., and Munson, R. S. (2013) *Acinetobacter baumannii* strain M2 produces type IV pili which play a role in natural transformation and twitching motility but not surface-associated motility. *MBio* **4,** e00360-13 Medline

15. Piepenbrink, K. H., Lillehoj, E., Harding, C. M., Labonte, J. W., Zuo, X., Rapp, C. A., Munson, R. S., Jr., Goldblum, S. E., Feldman, M. F., Gray, J. J., and Sundberg, E. J. (2016) Structural diversity in the type IV pili of multidrug-resistant *Acinetobacter*. *J. Biol. Chem.* **291,** 22924–22935 CrossRef Medline

16. Falagas, M. E., and Kopterides, P. (2006) Risk factors for the isolation of multidrug-resistant *Acinetobacter baumannii* and *Pseudomonas aeruginosa*: a systematic review of the literature. *J. Hosp. Infect.* **64,** 7–15 CrossRef Medline

17. Peleg, A. Y., Seifert, H., and Paterson, D. L. (2008) *Acinetobacter baumannii*: emergence of a successful pathogen. *Clin. Microbiol. Rev.* **21,** 538–582 CrossRef Medline

18. Poirel, L., Figueiredo, S., Cattoir, V., Carattoli, A., and Nordmann, P. (2008) *Acinetobacter radioresistens* as a silent source of carbapenem resistance for *Acinetobacter* spp. *Antimicrob. Agents Chemother.* **52,** 1252–1256 CrossRef Medline

19. Dijkshoorn, L., Nemec, A., and Seifert, H. (2007) An increasing threat in hospitals: multidrug-resistant *Acinetobacter baumannii*. *Nat. Rev. Microbiol.* **5,** 939–951 CrossRef Medline

20. Jones, A., Morgan, D., Walsh, A., Turton, J., Livermore, D., Pitt, T., Green, A., Gill, M., and Mortiboy, D. (2006) Importation of multidrug-resistant *Acinetobacter* spp. infections with casualties from Iraq. *Lancet Infect. Dis.* **6,** 317–318 CrossRef Medline

21. Harding, C. M., Kinsella, R. L., Palmer, L. D., Skaar, E. P., and Feldman, M. F. (2016) Medically relevant *Acinetobacter* species require a type II secretion system and specific membrane-associated chaperones for the export of multiple substrates and full virulence. *PLoS Pathog.* **12,** e1005391 CrossRef Medline

22. Howard, A., O'Donoghue, M., Feeney, A., and Sleator, R. D. (2012) *Acinetobacter baumannii*: an emerging opportunistic pathogen. *Virulence* **3,** 243–250 CrossRef Medline

23. Cosgaya, C., Marí-Almirall, M., Van Assche, A., Fernández-Orth, D., Mosqueda, N., Telli, M., Huys, G., Higgins, P. G., Seifert, H., Lievens, B., Roca, I., and Vila, J. (2016) *Acinetobacter dijkshoorniae* sp. nov., a member of the *Acinetobacter calcoaceticus–Acinetobacter baumannii* complex mainly recovered from clinical samples in different countries. *Int. J. Syst. Evol. Microbiol.* **66,** 4105–4111 CrossRef Medline

24. Nemec, A., Krizova, L., Maixnerova, M., Sedo, O., Brisse, S., and Higgins, P. G. (2015) *Acinetobacter seifertii* sp. nov., a member of the *Acinetobacter calcoaceticus–Acinetobacter baumannii* complex isolated from human clinical specimens. *Int. J. Syst. Evol. Microbiol.* **65,** 934–942 CrossRef Medline

25. Chang, H. C., Wei, Y. F., Dijkshoorn, L., Vaneechoutte, M., Tang, C. T., and Chang, T. C. (2005) Species-level identification of isolates of the *Acinetobacter calcoaceticus–Acinetobacter baumannii* complex by sequence analysis of the 16S–23S rRNA gene spacer region. *J. Clin. Microbiol.* **43,** 1632–1639 CrossRef Medline

26. Antunes, L. C., Visca, P., and Towner, K. J. (2014) *Acinetobacter baumannii*: evolution of a global pathogen. *Pathog. Dis.* **71,** 292–301 CrossRef Medline

27. Iacono, M., Villa, L., Fortini, D., Bordoni, R., Imperi, F., Bonnal, R. J., Sicheritz-Ponten, T., De Bellis, G., Visca, P., Cassone, A., and Carattoli, A. (2008) Whole-genome pyrosequencing of an epidemic multidrug-resistant *Acinetobacter baumannii* strain belonging to the European clone II group. *Antimicrob. Agents Chemother.* **52,** 2616–2625 CrossRef Medline

28. Jacobs, A. C., Thompson, M. G., Black, C. C., Kessler, J. L., Clark, L. P., McQueary, C. N., Gancz, H. Y., Corey, B. W., Moon, J. K., Si, Y., Owen, M. T., Hallock, J. D., Kwak, Y. I., Summers, A., Li, C. Z., *et al.* (2014) AB5075, a highly virulent isolate of *Acinetobacter baumannii*, as a model strain for the evaluation of pathogenesis and antimicrobial treatments. *MBio* **5,** e01076-14 Medline

29. Moon, A. F., Mueller, G. A., Zhong, X., and Pedersen, L. C. (2010) A synergistic approach to protein crystallization: combination of a fixed-arm carrier with surface entropy reduction. *Protein Sci.* **19,** 901–913 Medline

30. McCoy, A. J., Grosse-Kunstleve, R. W., Adams, P. D., Winn, M. D., Storoni, L. C., and Read, R. J. (2007) Phaser crystallographic software. *J Appl Crystallogr.* **40,** 658–674 CrossRef Medline

31. Adams, P. D., Afonine, P. V., Bunkóczi, G., Chen, V. B., Davis, I. W., Echols, N., Headd, J. J., Hung, L. W., Kapral, G. J., Grosse-Kunstleve, R. W., McCoy, A. J., Moriarty, N. W., Oeffner, R., Read, R. J., Richardson, D. C., *et al.* (2010) PHENIX: a comprehensive Python-based system for macromolecular structure solution. *Acta Crystallogr. D Biol. Crystallogr.* **66,** 213–221 CrossRef Medline

32. Adams, P. D., Afonine, P. V., Bunkóczi, G., Chen, V. B., Echols, N., Headd, J. J., Hung, L. W., Jain, S., Kapral, G. J., Grosse Kunstleve, R. W., McCoy, A. J., Moriarty, N. W., Oeffner, R. D., Read, R. J., Richardson, D. C., *et al.* (2011) The Phenix software for automated determination of macromolecular structures. *Methods* **55,** 94–106 CrossRef Medline

33. Adams, P. D., Grosse-Kunstleve, R. W., Hung, L. W., Ioerger, T. R., McCoy, A. J., Moriarty, N. W., Read, R. J., Sacchettini, J. C., Sauter, N. K., and Terwilliger, T. C. (2002) PHENIX: building new software for automated crystallographic structure determination. *Acta Crystallogr. D Biol. Crystallogr.* **58,** 1948–1954 CrossRef Medline

34. Emsley, P., and Cowtan, K. (2004) Coot: model-building tools for molecular graphics. *Acta Crystallogr. D Biol. Crystallogr.* **60,** 2126–2132 CrossRef Medline

35. Pettersen, E. F., Goddard, T. D., Huang, C. C., Couch, G. S., Greenblatt, D. M., Meng, E. C., and Ferrin, T. E. (2004) UCSF Chimera: a visualization system for exploratory research and analysis. *J. Comput. Chem.* **25,** 1605–1612 CrossRef Medline

SASBMB

36. Craig, L., Taylor, R. K., Pique, M. E., Adair, B. D., Arvai, A. S., Singh, M., Lloyd, S. J., Shin, D. S., Getzoff, E. D., Yeager, M., Forest, K. T., and Tainer, J. A. (2003) Type IV pilin structure and assembly: X-ray and EM analyses of *Vibrio cholerae* toxin-coregulated pilus and *Pseudomonas aeruginosa* PAK pilin. *Mol. Cell* **11,** 1139–1150 CrossRef Medline

37. Craig, L., Volkmann, N., Arvai, A. S., Pique, M. E., Yeager, M., Egelman, E. H., and Tainer, J. A. (2006) Type IV pilus structure by cryo-electron microscopy and crystallography: implications for pilus assembly and functions. *Mol. Cell* **23,** 651–662 CrossRef Medline

38. Chiang, P., and Burrows, L. L. (2003) Biofilm formation by hyperpiliated mutants of *Pseudomonas aeruginosa*. *J. Bacteriol.* **185,** 2374–2378 CrossRef Medline

39. Aranda, J., Poza, M., Pardo, B. G., Rumbo, S., Rumbo, C., Parreira, J. R., Rodríguez-Velo, P., and Bou, G. (2010) A rapid and simple method for constructing stable mutants of *Acinetobacter baumannii. BMC Microbiol.* **10,** 279 CrossRef Medline

40. Heydorn, A., Nielsen, A. T., Hentzer, M., Sternberg, C., Givskov, M., Ersbøll, B. K., and Molin, S. (2000) Quantification of biofilm structures by the novel computer program COMSTAT. *Microbiology* **146,** 2395–2407 CrossRef Medline

41. Schmid, B., Schindelin, J., Cardona, A., Longair, M., and Heisenberg, M. (2010) A high-level 3D visualization API for Java and ImageJ. *BMC Bioinformatics* **11,** 274 CrossRef Medline

42. Lillehoj, E. P., Hyun, S. W., Feng, C., Zhang, L., Liu, A., Guang, W., Nguyen, C., Luzina, I. G., Atamas, S. P., Passaniti, A., Twaddell, W. S., Puché, A. C., Wang, L. X., Cross, A. S., *et al.* (2012) NEU1 sialidase expressed in human airway epithelia regulates epidermal growth factor receptor (EGFR) and MUC1 protein signaling. *J. Biol. Chem.* **287,** 8214–8231 CrossRef Medline

43. Lillehoj, E. P., Hyun, S. W., Liu, A., Guang, W., Verceles, A. C., Luzina, I. G., Atamas, S. P., Kim, K. C., and Goldblum, S. E. (2015) NEU1 sialidase regulates membrane-tethered mucin (MUC1) ectodomain adhesiveness for *Pseudomonas aeruginosa* and decoy receptor release. *J. Biol. Chem.* **290,** 18316–18331 CrossRef Medline

44. Sievers, F., Wilm, A., Dineen, D., Gibson, T. J., Karplus, K., Li, W., Lopez, R., McWilliam, H., Remmert, M., Söding, J., Thompson, J. D., and Higgins, D. G. (2011) Fast, scalable generation of high-quality protein multiple sequence alignments using Clustal Omega. *Mol. Syst. Biol.* **7,** 539 Medline

45. Letunic, I., and Bork, P. (2016) Interactive tree of life (iTOL) v3: an online tool for the display and annotation of phylogenetic and other trees. *Nucleic Acids Res.* **44,** W242–W245 CrossRef Medline

46. Allison, T. M., Conrad, S., and Castric, P. (2015) The group I pilin glycan affects type IVa pilus hydrophobicity and twitching motility in *Pseudomonas aeruginosa* 1244. *Microbiology* **161,** 1780–1789 CrossRef Medline

47. Smedley, J. G., 3rd, Jewell, E., Roguskie, J., Horzempa, J., Syboldt, A., Stolz, D. B., and Castric, P. (2005) Influence of pilin glycosylation on *Pseudomonas aeruginosa* 1244 pilus function. *Infect. Immun.* **73,** 7922–7931 CrossRef Medline

48. Voisin, S., Kus, J. V., Houliston, S., St-Michael, F., Watson, D., Cvitkovitch, D. G., Kelly, J., Brisson, J. R., and Burrows, L. L. (2007) Glycosylation of *Pseudomonas aeruginosa* strain Pa5196 type IV pilins with mycobacterium-like α-1,5-linked D-Araf oligosaccharides. *J. Bacteriol.* **189,** 151–159 CrossRef Medline

49. Aas, F. E., Vik, A., Vedde, J., Koomey, M., and Egge-Jacobsen, W. (2007) *Neisseria gonorrhoeae* O-linked pilin glycosylation: functional analyses define both the biosynthetic pathway and glycan structure. *Mol. Microbiol.* **65,** 607–624 CrossRef Medline

50. Power, P. M., Seib, K. L., and Jennings, M. P. (2006) Pilin glycosylation in *Neisseria meningitidis* occurs by a similar pathway to wzy-dependent O-antigen biosynthesis in *Escherichia coli*. *Biochem. Biophys. Res. Commun.* **347,** 904–908 CrossRef Medline

51. Gault, J., Ferber, M., Machata, S., Imhaus, A. F., Malosse, C., Charles-Orszag, A., Millien, C., Bouvier, G., Bardiaux, B., Péhau-Arnaudet, G., Klinge, K., Podglajen, I., Ploy, M. C., Seifert, H. S., Nilges, M., *et al.* (2015) *Neisseria meningitidis* type IV pili composed of sequence invariable pilins are masked by multisite glycosylation. *PLoS Pathog.* **11,** e1005162 CrossRef Medline

52. Gellatly, S. L., and Hancock, R. E. (2013) *Pseudomonas aeruginosa*: new insights into pathogenesis and host defenses. *Pathog Dis.* **67,** 159–173 CrossRef Medline

53. McPherson, A. S., Dhungyel, O. P., and Whittington, R. J. (2017) Evaluation of genotypic and phenotypic protease virulence tests for *Dichelobacter nodosus* infection in sheep. *J. Clin. Microbiol.* **55,** 1313–1326 CrossRef Medline

54. Hartung, S., Arvai, A. S., Wood, T., Kolappan, S., Shin, D. S., Craig, L., and Tainer, J. A. (2011) Ultrahigh resolution and full-length pilin structures with insights for filament assembly, pathogenic functions, and vaccine potential. *J. Biol. Chem.* **286,** 44254–44265 CrossRef Medline

55. Wang, F., Coureuil, M., Osinski, T., Orlova, A., Altindal, T., Gesbert, G., Nassif, X., Egelman, E. H., Craig, L. (2017) Cryoelectron microscopy reconstructions of the *Pseudomonas aeruginosa* and *Neisseria gonorrhoeae* type IV pili at sub-nanometer resolution. *Structure* **25,** 1423–1435.e4 CrossRef Medline

56. Knutton, S., Shaw, R. K., Anantha, R. P., Donnenberg, M. S., and Zorgani, A. A. (1999) The type IV bundle-forming pilus of enteropathogenic *Escherichia coli* undergoes dramatic alterations in structure associated with bacterial adherence, aggregation and dispersal. *Mol. Microbiol.* **33,** 499–509 CrossRef Medline

57. Jude, B. A., and Taylor, R. K. (2011) The physical basis of type 4 pilus-mediated microcolony formation by *Vibrio cholerae* O1. *J. Struct. Biol.* **175,** 1–9 CrossRef Medline

58. Gebhardt, M. J., Gallagher, L. A., Jacobson, R. K., Usacheva, E. A., Peterson, L. R., Zurawski, D. V., and Shuman, H. A. (2015) Joint transcriptional control of virulence and resistance to antibiotic and environmental stress in *Acinetobacter baumannii. MBio* **6,** e01660-15 Medline

59. Tayabali, A. F., Nguyen, K. C., Shwed, P. S., Crosthwait, J., Coleman, G., and Seligy, V. L. (2012) Comparison of the virulence potential of *Acinetobacter* strains from clinical and environmental sources. *PLoS One* **7,** e37024 CrossRef Medline

60. Eijkelkamp, B. A., Stroeher, U. H., Hassan, K. A., Papadimitrious, M. S., Paulsen, I. T., and Brown, M. H. (2011) Adherence and motility characteristics of clinical *Acinetobacter baumannii* isolates. *FEMS Microbiol, Lett.* **323,** 44–51 CrossRef Medline

61. Harding, C. M., Nasr, M. A., Kinsella, R. L., Scott, N. E., Foster, L. J., Weber, B. S., Fiester, S. E., Actis, L. A., Tracy, E. N., Munson, R. S., Jr., and Feldman, M. F. (2015) *Acinetobacter* strains carry two functional oligosaccharyltransferases, one devoted exclusively to type IV pilin, and the other one dedicated to O-glycosylation of multiple proteins. *Mol. Microbiol.* **96,** 1023–1041 CrossRef Medline

62. Goeres, D. M., Loetterle, L. R., Hamilton, M. A., Murga, R., Kirby, D. W., and Donlan, R. M. (2005) Statistical assessment of a laboratory method for growing biofilms. *Microbiology* **151,** 757–762 CrossRef Medline

63. Greene, C., Wu, J., Rickard, A. H., and Xi, C. (2016) Evaluation of the ability of *Acinetobacter baumannii* to form biofilms on six different biomedical relevant surfaces. *Lett. Appl. Microbiol.* **63,** 233–239 CrossRef Medline

64. Nait Chabane, Y., Mlouka, M. B., Alexandre, S., Nicol, M., Marti, S., Pestel-Caron, M., Vila, J., Jouenne, T., and Dé, E. (2014) Virstatin inhibits biofilm formation and motility of *Acinetobacter baumannii. BMC Microbiol.* **14,** 62 CrossRef Medline

65. Oh, M. H., and Choi, C. H. (2015) Role of LuxIR homologue AnoIR in *Acinetobacter nosocomialis* and the effect of virstatin on the expression of anoR gene. *J. Microbiol. Biotechnol.* **25,** 1390–1400 CrossRef Medline

66. Pakharukova, N., Tuittila, M., Paavilainen, S., Malmi, H., Parilova, O., Teneberg, S., Knight, S. D., and Zavialov, A. V. (2018) Structural basis for *Acinetobacter baumannii* biofilm formation. *Proc. Natl. Acad. Sci. U.S.A.* **115,** 5558–5563 CrossRef Medline

67. Moon, K. H., Weber, B. S., and Feldman, M. F. (2017) Subinhibitory concentrations of trimethoprim and sulfamethoxazole prevent biofilm formation by *Acinetobacter baumannii* through inhibition of Csu pilus expression. *Antimicrob. Agents Chemother.* **61,** e00778-17 Medline

68. Marceau, M., Forest, K., Béretti, J. L., Tainer, J., and Nassif, X. (1998) Consequences of the loss of O-linked glycosylation of meningococcal type

IV pilin on piliation and pilus-mediated adhesion. *Mol. Microbiol.* **27,** 705–715 CrossRef Medline

69. Stimson, E., Virji, M., Makepeace, K., Dell, A., Morris, H. R., Payne, G., Saunders, J. R., Jennings, M. P., Barker, S., and Panico, M. (1995) Meningococcal pilin: a glycoprotein substituted with digalactosyl 2,4-diacetamido-2,4,6-trideoxyhexose. *Mol. Microbiol.* **17,** 1201–1214 CrossRef Medline

70. Biais, N., Ladoux, B., Higashi, D., So, M., and Sheetz, M. (2008) Cooperative retraction of bundled type IV pili enables nanonewton force generation. *PLoS Biol.* **6,** e87 CrossRef Medline

71. Marathe, R., Meel, C., Schmidt, N. C., Dewenter, L., Kurre, R., Greune, L., Schmidt, M. A., Müller, M. J., Lipowsky, R., Maier, B., and Klumpp, S. (2014) Bacterial twitching motility is coordinated by a two-dimensional tug-of-war with directional memory. *Nat. Commun.* **5,** 3759 CrossRef Medline

72. Vijayakumar, S., Rajenderan, S., Laishram, S., Anandan, S., Balaji, V., and Biswas, I. (2016) Biofilm formation and motility depend on the nature of the *Acinetobacter baumannii* clinical isolates. *Front. Public Health* **4,** 105 Medline

73. Sahl, J. W., Del Franco, M., Pournaras, S., Colman, R. E., Karah, N., Dijkshoorn, L., and Zarrilli, R. (2015) Phylogenetic and genomic diversity in isolates from the globally distributed *Acinetobacter baumannii* ST25 lineage. *Sci. Rep.* **5,** 15188 CrossRef Medline

74. Zhan, Y., Yan, Y., Zhang, W., Yu, H., Chen, M., Lu, W., Ping, S., Peng, Z., Yuan, M., Zhou, Z., Elmerich, C., and Lin, M. (2011) Genome sequence of *Acinetobacter calcoaceticus* PHEA-2, isolated from industry wastewater. *J. Bacteriol.* **193,** 2672–2673 CrossRef Medline

75. Wang, Y. C., Huang, T. W., Yang, Y. S., Kuo, S. C., Chen, C. T., Liu, C. P., Liu, Y. M., Chen, T. L., Chang, F. Y., Wu, S. H., How, C. K., and Lee, Y. T. (2018) Biofilm formation is not associated with worse outcome in *Acinetobacter baumannii* bacteraemic pneumonia. *Sci. Rep.* **8,** 7289 CrossRef Medline

76. Nguyen, Y., Sugiman-Marangos, S., Harvey, H., Bell, S. D., Charlton, C. L., Junop, M. S., and Burrows, L. L. (2015) *Pseudomonas aeruginosa* minor pilins prime type IVa pilus assembly and promote surface display of the PilY1 adhesin. *J. Biol. Chem.* **290,** 601–611 CrossRef Medline

77. Oki, H., Kawahara, K., Maruno, T., Imai, T., Muroga, Y., Fukakusa, S., Iwashita, T., Kobayashi, Y., Matsuda, S., Kodama, T., Iida, T., Yoshida, T., Ohkubo, T., and Nakamura, S. (2018) Interplay of a secreted protein with type IVb pilus for efficient enterotoxigenic. *Proc. Natl. Acad. Sci. U.S.A.* **115,** 7422–7427 CrossRef Medline

78. Harvey, H., Bondy-Denomy, J., Marquis, H., Sztanko, K. M., Davidson, A. R., and Burrows, L. L. (2018) *Pseudomonas aeruginosa* defends against phages through type IV pilus glycosylation. *Nat. Microbiol.* **3,** 47–52 CrossRef Medline

79. Rodgers, K., Arvidson, C. G., and Melville, S. (2011) Expression of a Clostridium perfringens type IV pilin by *Neisseria gonorrhoeae* mediates adherence to muscle cells. *Infect. Immun.* **79,** 3096–3105 CrossRef Medline

ASBMB

The structure of PilA from *Acinetobacter baumannii* AB5075 suggests a mechanism for functional specialization in *Acinetobacter* type IV pili

Leslie A. Ronish, Erik Lillehoj, James K. Fields, Eric J. Sundberg and Kurt H. Piepenbrink

---

Access the most updated version of this article at doi: 10.1074/jbc.RA118.005814

Alerts:
- When this article is cited
- When a correction for this article is posted

Click here to choose from all of JBC's e-mail alerts

This article cites 79 references, 23 of which can be accessed free at
http://www.jbc.org/content/294/1/218.full.html#ref-list-1